Spectrochimica Acta Part A 76 (2010) 376–383

Contents lists available at ScienceDirect

Spectrochimica Acta Part A: Molecular and Biomolecular Spectroscopy

journal homepage: www.elsevier.com/locate/saa

# Spectroscopic characterization and biological activity of Zn(II), Cd(II), Sn(II) and Pb(II) complexes with Schiff base derived from pyrrole-2-carboxaldehyde and 2-amino phenol

Bibhesh K. Singh[a,*], Anant Prakash[a], Hemant K. Rajour[b], Narendar Bhojak[c], Devjani Adhikari[a]

[a] Inorganic & Bioinorganic Research Lab, Department of Chemistry, Govt. Post Graduate College, Ranikhet 263645, Uttarakhand, India
[b] Department of Chemistry, Ramjas College, University of Delhi, Delhi 110007, India
[c] Department of Chemistry, Govt. Dunger College, MGS University, Bikaner, India

ARTICLE INFO

*Article history:*
Received 8 January 2010
Received in revised form 15 March 2010
Accepted 17 March 2010

*Keywords:*
Biological activities
Spectra
Schiff base
Metal complexes
Molecular modeling
Thermal studies

ABSTRACT

A new Schiff base *2-aminophenol-pyrrole-2-carboxaldehyde* and its Zn(II), Cd(II), Sn(II) and Pb(II) complexes have been synthesized and characterized by various physicochemical studies. Spectral studies (IR and $^{1}$H NMR) indicate deprotonation and coordination of phenolic oxygen along with binding of pyrrole nitrogen, azomethine nitrogen and anion with metal ions. The presence of lattice water molecule(s) has also been confirmed by TG/DTA studies. Mass spectrum explains the successive degradation of the molecular species in solution and justifies ML complexes. Kinetic and thermodynamic parameters were computed from the thermal data using Coats and Redfern method, which confirm first order kinetics. The bio-efficacy of the ligand and their complexes has been examined against the growth of bacteria *in vitro* to evaluate their antimicrobial potential. Molecular structures of the complexes have been optimized by MM2 calculations and suggest a tetrahedral geometry around metal ions.



## 1. Introduction

Schiff base ligands are considered "privileged ligands" because they are easily prepared by the condensation between aldehydes and amines. Stereogenic centers or other elements of chirality can be introduced in the synthetic design. Schiff base ligand is able to coordinate many different metals [1], and to stabilize them in various oxidation states. Structure–activity relationship of Schiff base compounds are studied due to their antitumor, antimicrobial and antiviral activities [2]. In recent years, because of new interesting applications found in the field of pesticides and medicine, the metal complexes with tridentate O, N, N types of alternative structures have attracted the attention of chemist. Various metal complexes with bi- and tridentate Schiff bases containing nitrogen and oxygen donor atoms play important role in biological system and represent interesting models for metalloenzymes, which efficiently catalyze the reduction of dinitrogen and dioxygen [3]. Schiff base complexes incorporating phenolic group as chelating moieties in the ligand are considered as models for executing important biological reactions and mimic the catalytic activities of metalloenzymes [4]. Furthermore, macrocyclic derivatives of these Schiff bases have many fundamental biological functions, such as photosynthesis and transport of oxygen in mammalian and other respiratory system [5].

In recent years metal compounds, which have a stable $d^{10}$ electronic configuration, have received a lot of attention in the fields of inorganic chemistry, biochemistry and environmental chemistry. About twenty zinc enzymes are known in which zinc is generally tetrahedrally four coordinate and bonded to hard donor atoms such as nitrogen [6]. Previously, it has been reported that zinc(II) and cadmium(II) complexes with Schiff bases type chelating ligand can be used as an effective emitting layer and showed photo physical properties [7]. Zinc complexes have been shown to be active as antitumor, anti-HIV and antimicrobial agents [8]. So, our interest is to establish spectroscopic bioactive model complexes of newly synthesized Schiff base with metal ions having $d^{10}$ configuration.

The present report deals with the synthesis, spectroscopic and thermal characterization of zinc(II), cadmium(II), tin(II) and lead(II) complexes with Schiff base derived from pyrrole-2-carboxaldehyde and 2-amino phenol and to examine their bio-efficacy of ligand as well as metal complexes. The free ligand and its complexes have been tested *in vitro* against *Escherichia coli* and *Staphylococcus aureus* bacteria with different concentrations, in order to assess their antimicrobial potential.

* Corresponding author. Tel.: +91 9760014796; fax: +91 5966220372.
*E-mail address:* bibheshksingh@yahoo.co.in (B.K. Singh).

1386-1425/$ – see front matter © 2010 Elsevier B.V. All rights reserved.
doi:10.1016/j.saa.2010.03.031

## 2. Experimental

### 2.1. Materials and methodology

All the chemicals used were of analytical grade and used as procured. Solvents used were of analytical grade and were purified by standard procedures. The stoichiometric analysis (C, H and N) of the complexes was performed using Elementar vario EL III (Germany) model. Metal contents were estimated on an AA-640-13 Shimadzu flame atomic absorption spectrophotometer in solutions prepared by decomposing the complex in hot concentrated $HNO_3$. The molar conductance at $10^{-3}$ M dilution was measured by Elico-Conductometer Bridge. The IR spectra were recorded on Perkin-Elmer FTIR spectrophotometer in KBr and polyethylene pellets. The UV–vis spectra were recorded in DMSO on Beckman DU-64 spectrophotometer with quartz cells of 1 cm path length and mass spectra (TOF-MS) were recorded on Waters (USA) KC-455 model with $ES^+$ mode in DMSO. $^1$H NMR spectra were recorded in DMSO solvent (solvent peak 3.8 ppm) on a Bruker Advance 400 instrument. Rigaku model 8150 thermoanalyser was used for simultaneous recording of TG–DTA curves at a heating rate of 10 min$^{-1}$. For TG, the instrument was calibrated using calcium oxalate, while for DTA, calibration was done using indium metal, both of which were supplied along with the instrument. A flat bed type aluminum crucible was used with α-alumina (99% pure) as the reference material for DTA. The number of decomposition steps was identified using TG. The activation energy and Arrhenius constant of the degradation process were obtained by Coats and Redfern method.

### 2.2. Biological activity: antibacterial screening

*In vitro* antibacterial activity of the compounds against *E. coli* and *S. aureus* were carried out using Muller Hinton Agar media (Hi media). The activity was carried out using paper disc method. Base plates were prepared by pouring 10 ml of autoclaved Muller Hinton agar into sterilized Petri dishes (9 mm diameter) and allowing them to settle. Molten autoclaved Muller Hinton that had been kept at 48 °C was incubated with a broth culture of the *E. coli* and *S. aureus* bacteria and then poured over the base plate. The discs were air dried and placed on the top of agar layer. The plates were incubated for 24–30 h and the inhibition zones (mm) were measured around each disc. As the organism grows, it forms a turbid layer, except in the region where the concentration of antibacterial agent is above the minimum inhibitory concentration, and a zone of inhibition is seen. The size of the inhibition zone depends upon the culture medium, incubation conditions, rate of diffusion and the concentration of the antibacterial agent. The solutions of all compounds were prepared in double distilled water and chloramphenicol was used as a reference.

### 2.3. Molecular modeling

3D molecular modeling of the proposed structure of the complexes was performed using HyperChem version 7.1 program package. The correct stereochemistry was assured through the manipulation and modification of the molecular coordinates to obtain reasonable low energy molecular geometries. The potential energy of the molecule was the sum of the following terms $(E) = E_{str} + E_{ang} + E_{tor} + E_{vdw} + E_{oop} + E_{ele}$, where all *E*s represent the energy values corresponding to the given types of interaction (kcal mol$^{-1}$). The subscripts str, ang, tor, vdw, oop and ele denote bond stretching, angle bonding, torsion, deformation, vanderwaals interactions, out of plain bending and electronic interaction, respectively. The molecular mechanics describe the application of classical mechanics to determination of molecular equilibrium structures. It enables the calculation of the total static energy of a molecule in terms of deviations from reference unstrained bond lengths, angles and torsions plus non-bonded interactions. On account of non-bonded interactions and also the chemical sense of each atom, treat the force field as a set of constants that have to be fixed by appeal to experiment or more rigorous calculations. It has been found that off-diagonal terms are usually largest when neighboring atoms are involved, and so we have to take account of non-bonded interactions, but only between next-nearest neighbors.

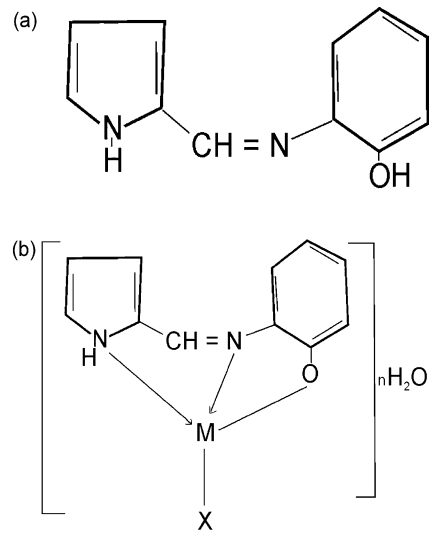


Where M = Zn(II), Pb(II), X= $CH_3CO_2$ and n =1
M = Cd(II), X = $NO_3$ and n = 1
M = Sn(II) ,X = Cl and n = 2

**Fig. 1.** (a) Structure of the ligand and (b) structure of the complex.

### 2.4. Synthesis of ligand and complexes

#### 2.4.1. Synthesis of 2-aminophenol-pyrrole-2-carboxaldehyde

Pyrrole-2-carboxaldehyde (30 mmol) was dissolved in absolute ethanol (20 ml) added dropwise to a solution of 2-aminophenol (30 mmol) in absolute ethanol (20 ml) with constant stirring. Stirring was continued with heating at 80 °C for 3 h. A brown colored powder was collected by vacuum filtration and dried overnight in vacuum. The yield and melting point of the product were determined.

#### 2.4.2. Synthesis of metal complexes

*2-Aminophenol-pyrrole-2-carboxaldehyde* (5 mmol) in 20 ml of absolute ethanol was added dropwise to a solution containing metal salts (5 mmol) in absolute alcohol (20 ml). The mixture was heated while being stirred. The precipitate was filtered, washed with cold alcohol and dried under vacuum over silica gel. The yield and melting point of each product were determined. The metal salts used were zinc acetate, cadmium nitrate, stannous chloride and lead acetate.

## 3. Results and discussion

The synthesized compounds (Fig. 1a and b) are crystalline and non-hygroscopic in nature. It is insoluble in water, partially soluble in ethanol but soluble in acetone, DMF and DMSO. Composition and identity of the assembled compounds were deduced from elemental analyses, spectroscopic techniques (IR, UV–vis, $^1$H NMR, TOF-MS) and thermal studies. The analytical data of the complexes indicated 1:1 metal to ligand stoichiometry. Possible composition

**Table 1**
Analytical and physical data of ligands and their complexes.

| S. no | Compounds (empirical formula) | Colors | MP (°C) | Yield (%) | Elemental analysis (found/calc.) | | | |
|---|---|---|---|---|---|---|---|---|
| | | | | | C | H | N | M |
| 1 | **L** ($C_{11}H_{10}N_2$) | Brown | 130 | 84 | 70.93 (70.96) | 5.39 (5.37) | 15.09 (15.05) | – |
| 2 | **I** ($C_{13}H_{14}O_4N_2Zn$) | Light yellow | 190 | 83 | 47.63 (47.65) | 4.26 (4.27) | 8.53 (8.55) | 19.98 (19.96) |
| 3 | **II** ($C_{11}H_{11}O_5N_3Cd$) | Light brown | 200 | 81 | 34.95 (34.97) | 2.90 (2.91) | 11.07 (11.12) | 29.82 (29.78) |
| 4 | **III** ($C_{11}H_{13}O_3N_2ClSn$) | Cream | 175 | 86 | 35.19 (35.20) | 3.45 (3.46) | 7.44 (7.46) | 31.63 (31.65) |
| 5 | **IV** ($C_{13}H_{14}O_4N_2Pb$) | Light yellow | 360 | 83 | 33.20 (33.24) | 2.97 (2.98) | 5.92 (5.96) | 44.16 (44.15) |

**Table 2**
Spectroscopic data (IR, $^1$H NMR, UV) of ligand and complexes.

| S. No | Compound | Infrared ($cm^{-1}$) | | | $^1$HNMR $\delta$ ppm | | UV (nm) |
|---|---|---|---|---|---|---|---|
| | | $\nu$(C=N) | $\nu$(M–N) | Others | (CH=N) | Others | |
| 1 | **L** | 1630(s) | – | – | 8.75 | | 252, 318 |
| 2 | **I** | 1620(s) | 527(s) | [$\nu_{as}(CO_2)$1632(s)], [$\nu_s(CO_2)$ 1412(s)] | 8.11 | 2.99 (acetate gr) | 274, 320 |
| 3 | **II** | 1613(s) | 536(s) | $\nu(NO_3)$ [1384,1272,731,965] | 8.27 | | 276, 332 |
| 4 | **III** | 1625(s) | 490(s) | $\nu$(Sn–Cl) 365(s) | 8.52 | | 278, 345 |
| 5 | **IV** | 1629(s) | 530(s) | [$\nu_{as}(CO_2)$:1620(s)], [$\nu_s(CO_2)$:1418(s)] | 7.75 | 2.49–8.08 (acetate gr) | 275, 340 |

of the complexes (Table 1) was calculated and compared with the experimental values and the molar conductivities of complexes have been studied in DMSO of $10^{-3}$ M of their solutions at room temperature. It is concluded from the results that all complexes are found to have molar conductance values in the range of 20–25 $ohm^{-1}\,mol^{-1}\,cm^2$. These low values of conductance are indicating the non-electrolytic nature of these complexes [9].

### 3.1. Spectroscopic studies

#### 3.1.1. Infrared spectra and mode of bonding

In the absence of a powerful technique such as X-ray crystallography, infrared spectra have proven to be the most suitable technique to give enough information's to elucidate the nature of bonding of the ligand to the metal ions. The significant infrared bands of the Schiff base and their metal complexes are given in Table 2. The observed bands may be classified into those originating from the ligand and those arising from the bonds formed between metal ions and the coordinating sites (Fig. 2: IR spectrum of complex **II**). Infrared spectrum of the ligand, shows a broad band between 3200 and 3450 $cm^{-1}$, which can be attributed to phenolic OH group. This band disappears in all complexes, which can be attributed to the involvement of phenolic OH group in coordination. The involvement of deprotonated phenolic moiety in complexes is confirmed by the shift of $\nu$(C–O) stretching band observed at 1283 $cm^{-1}$ in the free ligand to a lower frequency to the extent 10–20 $cm^{-1}$ [10]. The shift of $\nu$(C–O) band at 1283 $cm^{-1}$ to a lower frequency suggests the weakening of $\nu$(C–O) and formation of stronger M–O bond. The free Schiff base ligand showed a strong band at 1630 $cm^{-1}$, which is characteristic of the azomethine (–HC=N) group [11]. Coordination of the Schiff base to the metal through the nitrogen atom is expected to reduce electron density in the azomethine link and lower the $\gamma_{C=N}$ absorption frequency. The band due to $\gamma_{C=N}$ is shifted to lower frequencies and appears around 1613–1625 $cm^{-1}$, indicating coordination of the azomethine nitrogen to metal ions [12]. The coordination of the azomethine nitrogen is further supported by the appearance of bands in the range of 490–540 $cm^{-1}$ due to $\gamma_{M-N}$. The N–H stretching frequency at 3135–2900 $cm^{-1}$ in the free ligand showed considerable shift in all the complexes, indicating participation of this N–H group in complexes [13]. All complexes showed broad

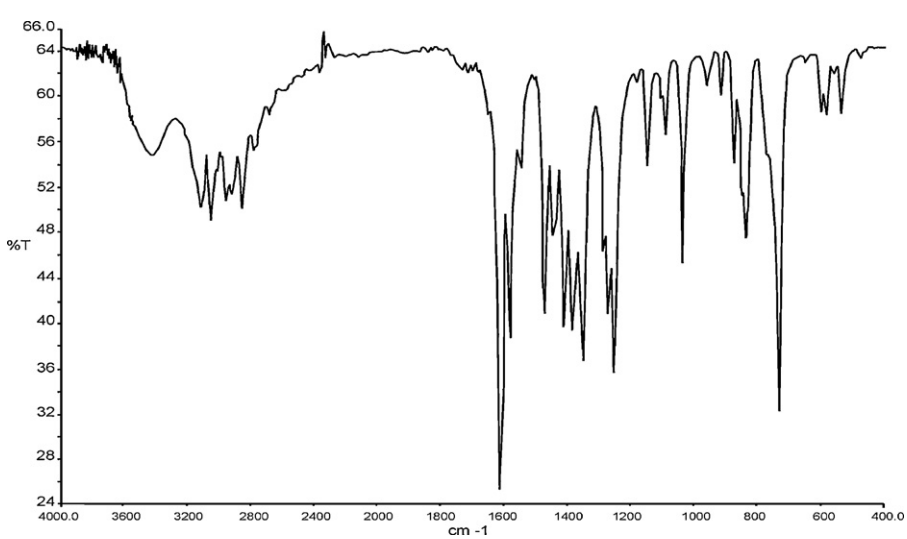


**Fig. 2.** IR spectrum of complex **II**.

band around 3400 $cm^{-1}$ due to $\nu$(OH) from water molecules. This band is absent in the ligand. This has been confirmed with thermal studies.

The complex **I** has bands at 1632(s) $cm^{-1}$ and 1412(s) $cm^{-1}$ which can be assigned to $\nu_{as}(CO_2)$ and $\nu_s(CO_2)$ fundamental stretching bands respectively, which are in agreement with the acetate groups being monodentate [14] because the difference $\Delta$ [$\Delta = \nu_{as}(CO_2) - \nu_s(CO_2)$] is 1632–1412 = 220 $cm^{-1}$. The band at 1412 $cm^{-1}$ is due to $\nu_s(CO_2)$ mode of bonding of acetate. Similarly in complex **IV** bands at 1620(s) $cm^{-1}$ and 1418(s) $cm^{-1}$ have been assigned to $\nu_{as}(CO_2)$ and $\nu_s(CO_2)$ fundamental stretching bands respectively indicating monodentate coordination of acetate group.

In addition to the modified slightly on account of coordination, infrared spectra of the complex **II** show absorption bands at ca. 1272, 1094, 731, 1384, 965, 1038 $cm^{-1}$ due to coordinated nitrato group. These bands are assigned as $\nu_1$, $\nu_2$, $\nu_3$, $\nu_4$, $\nu_5$, $\nu_6$ modes respectively, and their frequencies are consistent with those associated with terminally bonded monodentate nitrato group [15]. In addition to these two weak bands with a separation of ca. 12 $cm^{-1}$ appear in the 1800–1700 $cm^{-1}$ region indicating clearly the exclusive presence of terminal monodentate nitrato group [16].

In complex **III,** the $\nu$(Sn–Cl) band is observed at 365(s) $cm^{-1}$ which showed terminal rather than bridging chlorine [14].

### 3.1.2. $^1$H NMR spectra and electronic spectra

The $^1$H NMR spectrum of the ligand and the complexes were recorded to confirm the binding of the Schiff base to the metal ions (Fig. 3a and b). The spectra of the complexes showed a singlet in the region $\delta$ 7.75–8.52 ppm, which has been assigned to the azomethine proton (–HC=N) (Table 2). The position of the azomethine signal in the complexes is downfield in comparison with that of the free ligand, suggesting deshielding of the azomethine proton due to its coordination to metal ions through the azomethine nitrogen. In the region 6.70–7.90 ppm were assigned chemical shifts for hydrogen of symmetrical aromatic ring of ligand and peaks in the region 6.2–6.7 ppm were assigned chemical shift of pyrrole hydrogen [17]. A new peak at $\delta$ 11.76 ppm, characteristic of intramolecular hydrogen bonded phenolic OH group is disappeared in the spectra of the complexes indicating deprotonation of phenolic proton and confirming coordination through phenolic oxygen. In complexes the peak in the region of 3.0–3.5 ppm were assigned for coordinated water and another peak at 4.5 ppm especially in DMSO solvent (Fig. 3b: $^1$H NMR spectrum of complex **IV**) confirms the hydrogen bonded water molecule [17]. A new peak in the region $\delta$ 2.5–3.0 ppm, characteristic of acetate groups (6H) present in the spectrum of complexes **I** and **IV** is absent in the spectrum of the ligand. A weak peak in the region $\delta$ 3.1–3.3 ppm in complexes **I** and **IV** may be explained with the intramolecular hydrogen bonding acetate group with the coordinated water molecule [17].

The electronic spectra (Table 2) of the DMSO solutions of the free ligand, recorded in the 250–800 nm exhibit bands in the range 250–280 and 300–340 nm assigned to the $\pi \rightarrow \pi^*$ and $n \rightarrow \pi^*$ transitions respectively of the azomethine group and it is shifted to longer wavelength on coordination through azomethine nitrogen in the complexes [18].

### 3.1.3. TOF-mass spectra

Mass spectrometry has been successfully used to investigate molecular species in solution [19]. The pattern of mass spectrum gives an impression of the successive degradation of the target compound with the series of peaks corresponding to the various fragments. Their intensity gives an idea of stability of fragments. The recorded mass spectra of the ligand and their metal complexes

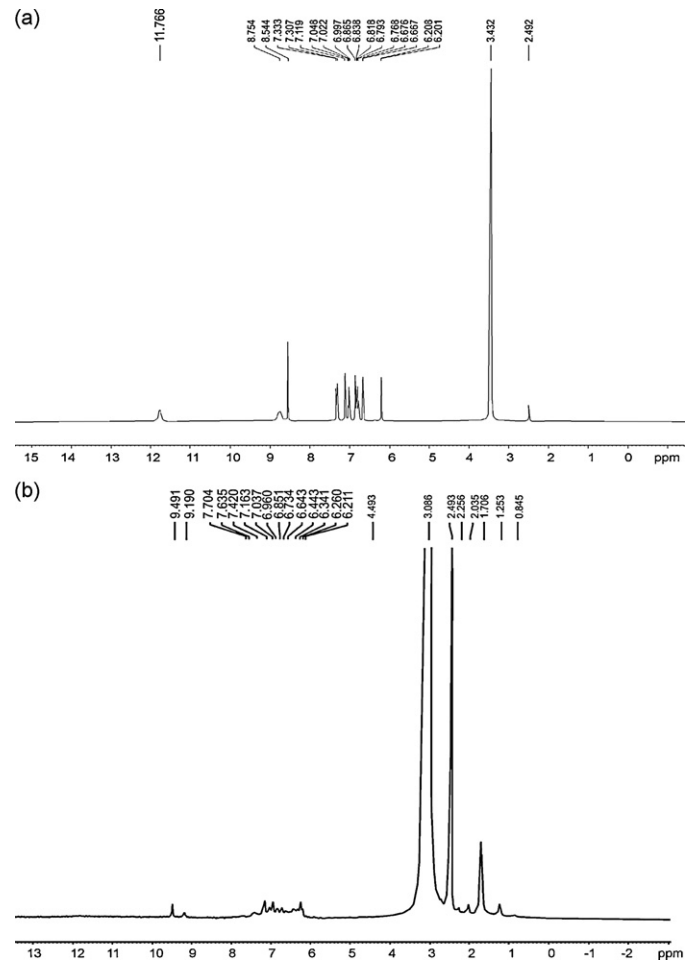


**Fig. 3.** (a) $^1$HNMR spectrum of ligand and (b) $^1$HNMR spectrum of complex **IV**.

of molecular ion peaks have been used to confirm the proposed formula (Fig. 4a–d). The mass spectrum of ligand having peaks at 186{100% *m*/*z*} and 145{34% *m*/*z*}, respectively, to the molecular ion peak $[M]^+$+1 and $[C_9H_8NO]^+$, confirming purity of the ligand. The mass spectra of complex **I** have a prominent peaks like 329{50% *m*/*z*} showing molecular ion peak, peak at 228/229{74% *m*/*z*} is $\{[M]^+ - H_2O - ZnO\} - 1$, peak at 187{90% *m*/*z*} is $[L]^+$+2 and peak at 146{63% *m*/*z*} is $[C_9H_8NO]^+$ respectively, showing usual degradation pattern. In complex **II** the degradation pattern again showing similar trends like peak at 379 {42% *m*/*z*} is molecular ion peak and subsequent peaks are 250{40% *m*/*z*} of $[M]^+ - [CdO]$, 186{36% *m*/*z*} of $[LH]^+$ and 146 {40% *m*/*z*} of $[C_9H_8NO]^+$ respectively. In complex **III**, the degradation pattern have prominent peaks at 186{100% *m*/*z*} and 145{47% *m*/*z*} showing $[LH]^+$ and $[C_9H_8NO]^+$ respectively. The complex **IV** shows degradation peak at 469/470 {35% *m*/*z*} of molecular ion peak, 450 {100% *m*/*z*} is $\{[M]^+ - H_2O\}$, 388{37% *m*/*z*} is $\{[M]^+ - H_2O - CH_3CO_2\}$ and 183{20% *m*/*z*} is $[LH]^+$ respectively. Likewise peaks attributable to monomeric species as $[M(L)]^+$ and $[HL]^+$ are usually present in the mass spectra of these systems [20]. Last two fragments at 185/186 and 146/145 are $[LH]^+$ and $[C_9H_8NO]^+$ of ligand peaks that appear in all these complexes showing similar pattern of degradation.

## 3.2. Thermal decomposition kinetics

Recently, there has been increasing interest in determining the rate-dependent parameters of solid-state non-isothermal decomposition reactions by analysis of TG curves [21]. Thermogravimetric

(TG) and differential thermogravimetric analysis (DTA) were carried out for Zn(II), Cd(II), Sn(II) and Pb(II)–Schiff base complexes in ambient condition (Fig. 5a–d). The correlations between the different decomposition steps of the complexes with the corresponding weight losses are reported in Table 3.The final product of decomposition at 810 K corresponds to the formation of metal oxide as end product, which was confirmed by comparing the observed/estimated and the calculated mass of the pyrolysis product.

The kinetic analysis parameters such as activation energy ($\Delta E^*$), enthalpy of activation ($\Delta H^*$), entropy of activation ($\Delta S^*$), free energy change of decomposition ($\Delta G^*$) were evaluated graphically

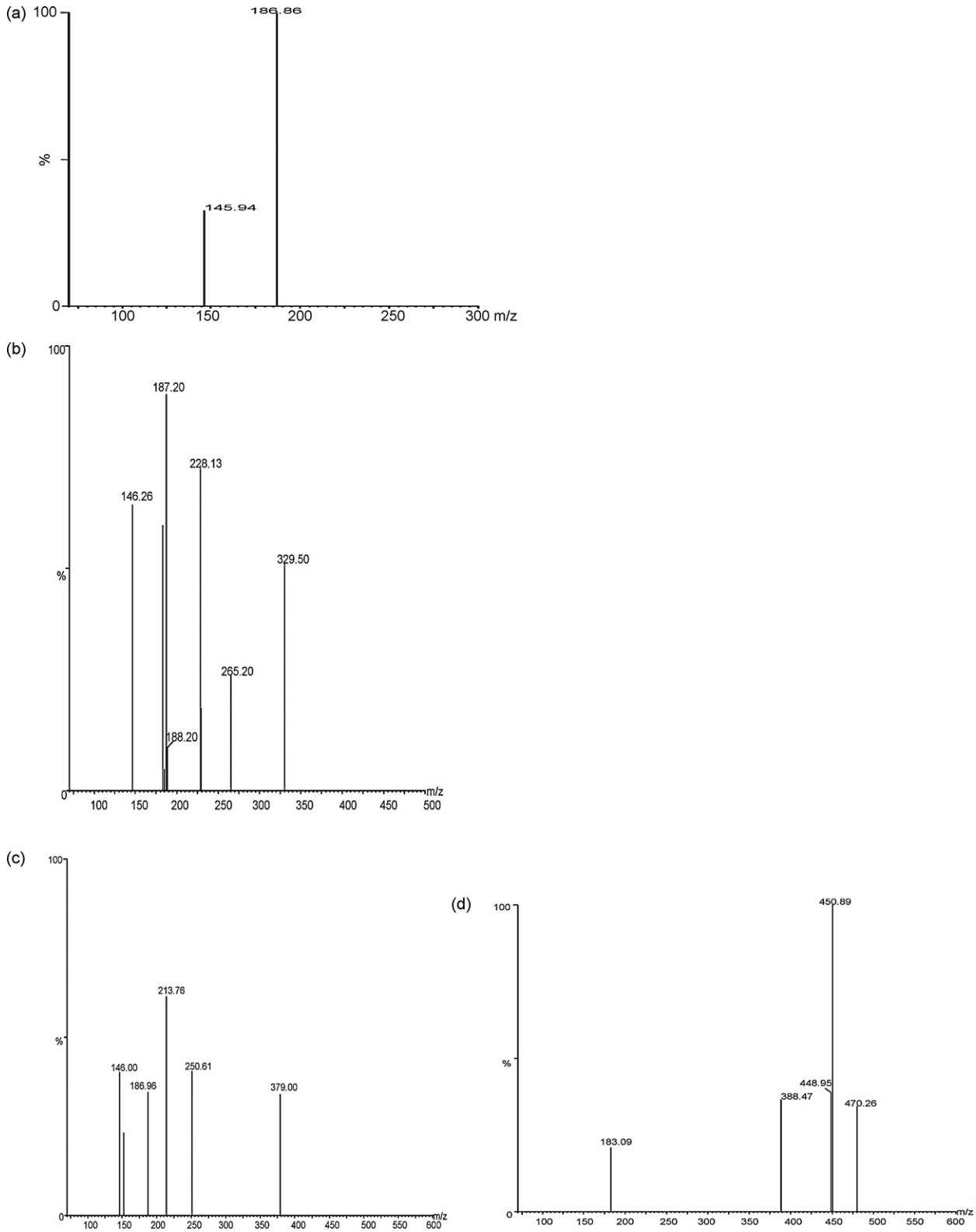


**Fig. 4.** (a) Mass spectrum of ligand; (b) mass spectrum of complex **I**; (c) mass spectrum of complex **II** and (d) mass spectrum of complex **IV**.

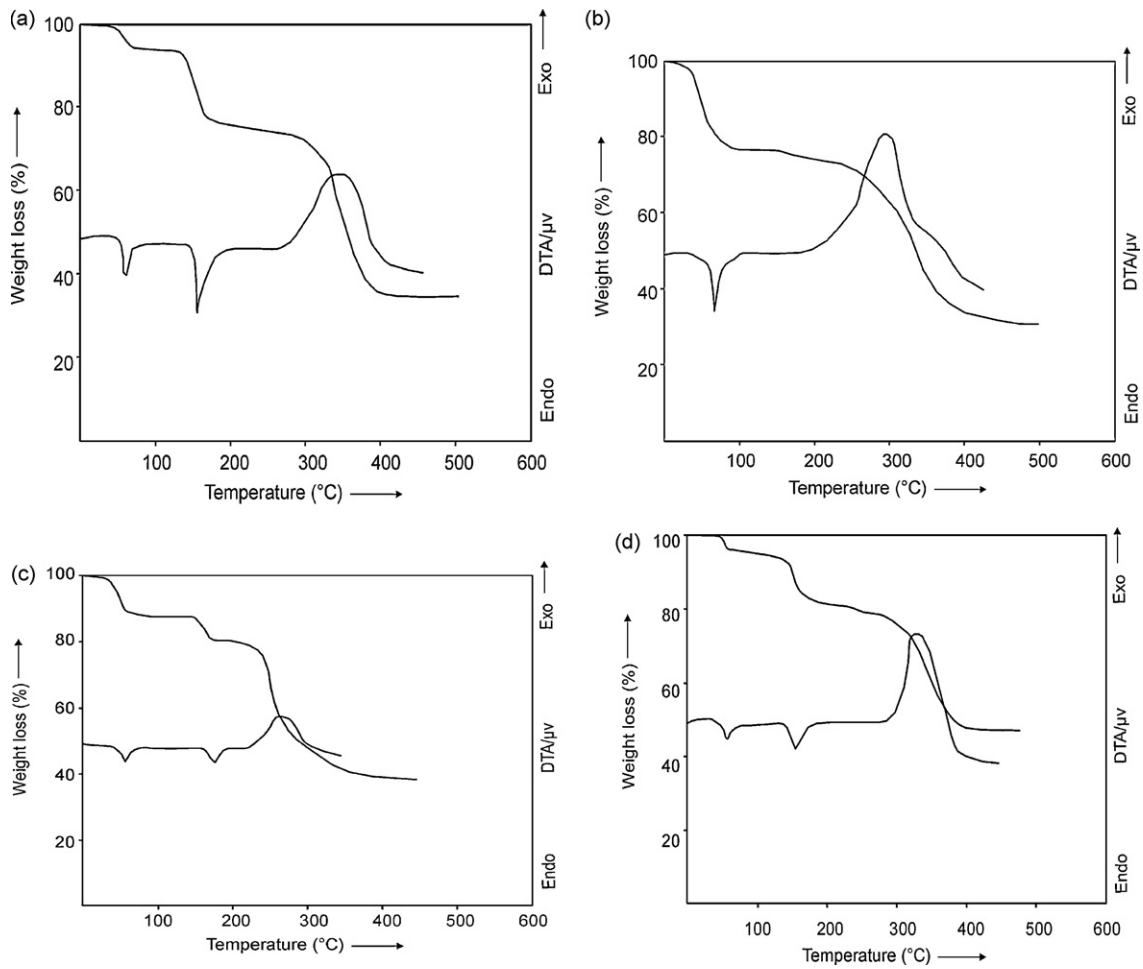


**Fig. 5.** (a) TG/DTA curve of complex **I**; (b) TG/DTA curve of complex **II**; (c) TG/DTA curve of complex **III** and (d) TG/DTA curve of complex **IV**.

by employing the Coats–Redfern relation [22].

$$\log\left[-\log\left(\frac{1-\alpha}{T^2}\right)\right] = \log\left[\frac{AR}{\theta E^*(1-2RT/E^*)}\right] - \frac{E^*}{2.303RT} \quad (1)$$

where $\alpha$ is the mass loss up to the temperature $T$, $R$ the gas constant, $E^*$ the activation energy in J mol$^{-1}$, $\theta$ the linear heating rate and $(1-2RT/E^*) \approx 1$. A plot of left hand side of Eq. (1) against $1/T$ gives a slope from which $E^*$ was calculated and $A$ (Arrhenius constant) was determined from the intercept. From relevant data, linearization plots confirm first order kinetics. It has been found that $E^*$ values for complexes > ligand.

The entropy of activation ($\Delta S^*$) and the free energy change of activation ($\Delta G^*$) were calculated using Eqs. (2) and (3):

$$\Delta S^* \,(\mathrm{JK^{-1}\,mol^{-1}}) = 2.303R\left[\log\left(\frac{Ah}{kT}\right)\right] \quad (2)$$

$$\Delta G^* (\mathrm{J\,mol^{-1}}) = \Delta H^* - T\Delta S^* \quad (3)$$

where $k$ and $h$ are the Boltzman and Plank constants, respectively. The calculated values of $\Delta E^*$, $A$, $\Delta S^*$ and $\Delta G^*$ for the decomposition steps of the complexes are given in Table 4. According to the kinetic data obtained from the TG curves, all the complexes have negative entropy, which indicates that the complexes are formed spontaneously. The negative entropy also indicates a more ordered

**Table 3**
Thermo analytical data.

| Complex | Step | $TG_{range}$/K | $DTA_{max}$/K thermal effect | Massloss cal (obs) (%) | Assignment | Metallic residue |
|---|---|---|---|---|---|---|
| **I** | I | 318–348 | 333 Endo | 5.48 (5.47) | $H_2O$ | |
| | II | 413–448 | 428 Endo | 17.97 (17.95) | $CH_4 + CO_2$ | |
| | III | 553–683 | 623 Exo | 41.18 (41.20) | Organic moiety | ZnO |
| **II** | I | 315–363 | 338 Endo | 21.16 (21.19) | $H_2O + [NO_2 + O]$ | |
| | II | 473–698 | 568 Exo | 44.98 (44.95) | Organic moiety | CdO |
| **III** | I | 303–343 | 328 Endo | 9.57 (9.60) | $2H_2O$ | |
| | II | 423–453 | 445 Endo | 9.70 (9.72) | HCl | |
| | III | 493–633 | 538 Exo | 39.61 (39.60) | Organic moiety | SnO |
| **IV** | I | 303–343 | 328 Endo | 3.83 (3.80) | $H_2O + [NO_2 + O]$ | |
| | II | 413–449 | 433 Endo | 12.55 (12.59) | $CH_4 + CO_2$ | |
| | III | 553–673 | 603 Exo | 36.15 (36.18) | Organic moiety | PbO |

**Table 4**
Thermodynamic activation parameters.

| Complex | Order | Step | $E^*$ (J mol$^{-1}$) | $A \times 10^5$ (s$^{-1}$) | $\Delta S^*$ (J K$^{-1}$ mol$^{-1}$) | $\Delta H^*$ (J mol$^{-1}$) | $\Delta G^*$(kJ mol$^{-1}$) |
|---|---|---|---|---|---|---|---|
| **I** | 1 | I | 41.10 | 1.35 | −147.37 | 72.02 | 49.14 |
| | | II | 39.96 | 0.99 | −152.02 | 98.64 | 65.16 |
| | | III | 41.55 | 0.73 | −157.67 | 243.89 | 98.47 |
| **II** | 1 | I | 55.74 | 3.61 | −139.32 | 143.32 | 47.23 |
| | | II | 53.24 | 1.93 | −148.83 | 476.89 | 85.01 |
| **III** | 1 | I | 60.06 | 3.51 | −139.31 | 98.22 | 45.79 |
| | | II | 79.00 | 4.34 | −140.13 | 182.67 | 62.96 |
| | | II | 60.52 | 2.14 | −147.52 | 317.81 | 79.68 |
| **IV** | 1 | I | 50.96 | 3.08 | −140.39 | 142.52 | 46.18 |
| | | II | 47.78 | 2.05 | −146.08 | 159.06 | 63.41 |
| | | III | 47.78 | 1.47 | −151.59 | 572.34 | 91.98 |

activated state that may be possible through the chemisorptions of oxygen and other decomposition products. The negative values of the entropies of activation are compensated by the values of the enthalpies of activation, leading to almost the same values for the free energies of activation [23].

### 3.3. Molecular structure and analysis of bonding modes

Molecular mechanics attempt to reproduce molecular geometries, energies and other features by adjusting bond length, bond angles and torsion angles to equilibrium values that are dependent on the hybridization of an atom and its bonding scheme. In order to obtain estimates of structural details of these complexes, we have optimized the molecular structure of complexes. Energy minimization was repeated several times to find the global minimum. The energy minimization value for tetrahedral and without restricting the structure for the complex **II** is almost same i.e., 32.674 kcal mol$^{-1}$. This supports tetrahedral geometry of the metal complex [24]. The optimized molecular structure and bond length of complex **II** are represented in Fig. 6.

### 3.4. Biological studies

The bacteriological effect of *2-aminophenol-pyrrole-2-carboxaldehyde* containing pyrrole-2-carboxaldehyde and 2-amino phenol moiety and its metal complexes were determined against two bacterium under different concentrations, as described in Section 2. The agar well-diffusion method was employed for the bacteria with respect to chloramphenicol as standard drug. The results showed that some compounds are very effective on some microorganisms (Fig. 7a and b). The ligand and complexes **I** and **II** exhibited high activity against *E. coli* (100 ppm) and others show very effective against *S. aureus* (100 ppm) bacteria. The zinc complex showed better activity than other metal complexes for both microorganisms. The activity of any compound is a complex combination of steric, electronic and pharmacokinetic factors. A possible explanation for the toxicity of the complexes has been postulated in the light of chelation theory. The presence of N and O donor groups in the ligand and its metal complexes inhibited enzyme production because enzymes that require free hydroxyl group for their activity appear to be especially susceptible to deactivation by the metal ion of complexes. Chelation reduces the polarity of the central ion from partial sharing of its positive charge with the donor groups; π-electron delocalization in this chelating

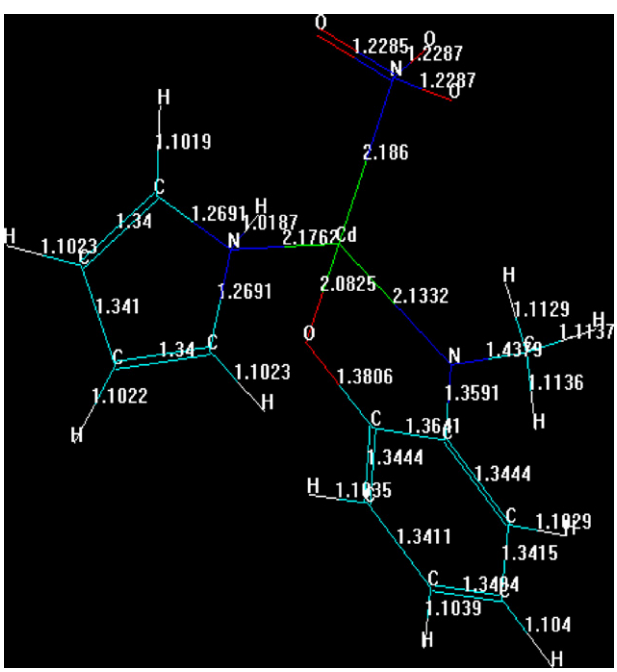


**Fig. 6.** Optimized structure of complex **II**.

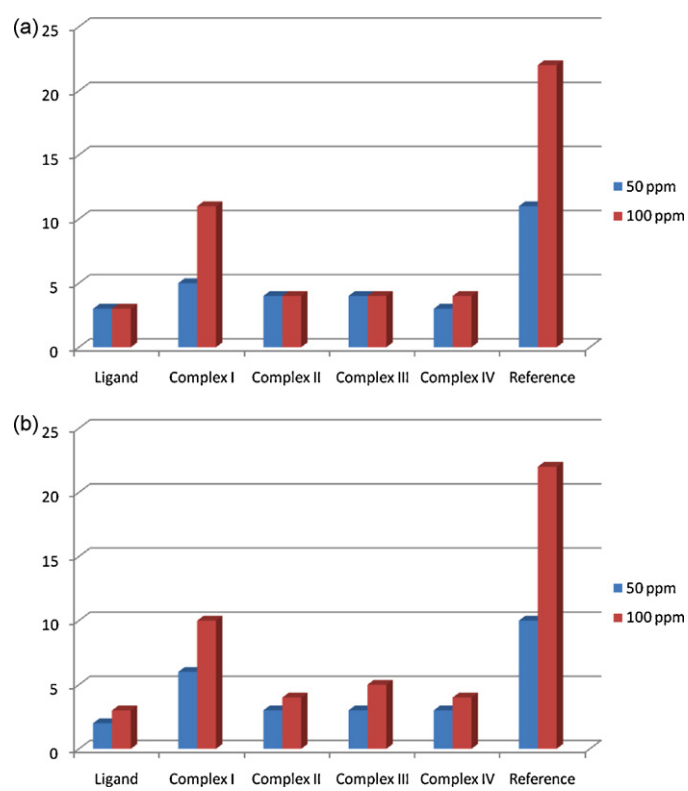


**Fig. 7.** (a) Effect of different concentrations of ligand and complexes with *Escherichia coli* and (b) effect of concentration of ligand and complexes with *Staphylococcus aureus*.

ring also increases the lipophilic nature of the central atom, favoring permeation through the lipid layer of the membrane [25]. All the metal complexes are more toxic than the ligand.

## 4. Conclusions

A new bioactive *2-aminophenol-pyrrole-2-carboxaldehyde Schiff* base as deprotonation and coordination of phenolic oxygen with metal ions along with binding with pyrrole nitrogen, azomethine nitrogen and anion with tetrahedral geometry were prepared and their structures were determined with spectroscopic and thermal studies. Molecular modeling has been used to optimize the structure of the metal complexes and its bond length has been determined.

## Acknowledgement

B K Singh and A Prakash are thankful to Council of Scientific and industrial Research, New Delhi, India for financial assistance under research grant scheme.

## References

[1] (a) P.G. Cozzi, Chem. Soc. Rev. 33 (2004) 410–421;
(b) S.A. Sallam, Trans. Met. Chem. 31 (2006) 46–55.
[2] (a) S. Ren, R. Wang, K. Komatsu, P. Bonaz-Krause, Y. Zyrianov, C.E. McKenna, C. Csipke, Z.A. Tokes, E.J. Lien, J. Med. Chem. 45 (2002) 410–419;
(b) P. Panneerselvam, R.R. Nair, G. Vijayalakshmi, E.H. Subramanian, S.K. Sridhar, Eur. J. Med. Chem. 40 (2005) 225–229;
(c) S.N. Pandeya, D. Sriram, G. Nath, E. DeClercq, Eur. J. Pharmacol. 9 (1999) 25–31;
(d) P. Vicini, A. Geronikaki, M. Incerti, B. Busonera, g. Poni, C.A. Cabrasc, P.L. Collac, Bioorg. Med. Chem. 11 (2003) 4785–4789.
[3] (a) V.T. Kasumov, S. Ozalp-Yaman, E. Tas, Spectrochim. Acta A 62 (2005) 716–720;
(b) J. Frausto da Silva, R. Williams, The Biological Chemistry of the Elements, Clarendon Press, Oxford, 1991;
(c) W. Kaim, B. Schwederski, Bioinorganic Chemistry: Inorganic Elements in the Chemistry of Life, Wiley, New York, 1996.
[4] A.A. Khandar, S.A. Hosseini-Yazdi, S.A. Zarei, U.M. Rabie, Inorg. Chim. Acta 358 (2005) 3211–3217.
[5] (a) P.K. Coughlin, S.J. Lippard, J. Am. Chem. Soc. 106 (1984) 2328–2336;
(b) Y.P. Cai, C.Y. Su, A.W. Xu, B.S. Kang, Y.X. Tong, H.Q. Liu, S. Jie, Polyhedron 20 (2001) 657–662.
[6] F. Marchettic, C. Pettinari, R. Pettinari, A. Cingolani, D. Leanesi, A. Lorenotti, Polyhedron 18 (1999) 3041–3050.
[7] T. Kawamoto, M. Nishiwaki, Y. Tsunekawa, K. Nozaki, T. Konno, Inorg. Chem. 47 (2008) 3095–3104.
[8] (a) X. Sheng, X. Guo, X.M. Lu, G.Y. Lu, Y. Shao, F. Liu, Q. Xu, Bioconjugate Chem. 19 (2008) 490–498;
(b) M.T. Kaczmareka, R. Jastrzaba, E. Holderna-Kedziab, W. Radecka-Paryzek, Inorg. Chim. Acta (2009), doi:10.1016/j.ica.2009.02.012;
(c) A.R. Cowley, J. Davis, J.R. Dilworth, P.S. Donnelly, R. Dobson, A. Nightingale, J.M. Peach, B. Shore, D. Kerr, L. Seymour, Chem. Commun. (2005) 845–847;
(d) T. Koike, M. Takashige, E. Kimura, H. Fujioka, M. Shiro, Chem. Eur. J. 2 (1996) 617–623.
[9] U.M. Rabie, A.S.A. Assran, M.H.M. Abou-El-wap, J. Mol. Struct. 872 (2008) 113–122.
[10] M.M. Omar, G.G. Mohamed, Spectrochim. Acta A61 (2005) 929–936.
[11] R. Ramesh, S. Maheshwaram, J. Inorg. Biochem. 96 (2003) 457–461.
[12] S.A. Ali, A.A. Soliman, M.M. Aboaly, R.M. Ramadan, J. Coord. Chem. 55 (2002) 1161–1170.
[13] S. Chandra, U. Kumar, Spectrochim. Acta A 60 (2004) 2825–2829.
[14] K. Nakamoto, Infrared and Raman Spectra of Inorganic and Coordination Compounds, Wiley, New York, 1978.
[15] (a) C.C. Addison, D. Sultons, Prog. Inorg. Chem. 8 (1967) 195;
(b) C.C. Addision, N. Logan, S.C. Wallwork, C.D. Garner, Quart. Rev. Chem. Soc. 25 (1971) 289.
[16] (a) A.B.P. Lever, E. Manto Vani, B.S. Ramaswami, Can. J. Chem. 49 (1971) 1957–1961;
(b) M. Choca, J.R. Ferraro, K. Nakamoto, J. Chem Soc. A (1972) 2297–2301.
[17] R.M. Silverstein, F.X. Webster, Spectrometric Identification of Organic Compounds, Sixth Edition, Wiley-India, 2007.
[18] A. Garg, J.P. Tondon, Transition Met. Chem. 12 (1987) 212–214.
[19] (a) J. Sanmartin, F. Novio, A.M. Garcia-Deibe, M. Fondo, N. Ocampo, M.R. Bermejo, Polyhedron 25 (2006) 1714–1722;
(b) I. Beloso, J. Castro, J.A. Garcia-Vazquez, P. Perez-Lourido, J. Romero, A. Sousa, Polyhedron 22 (2003) 1099–1111;
(c) B.K. Singh, A. Prakash, D. Adhikari, Spectrochim. Acta A 74 (2009) 657–664.
[20] N. Yoshida, K. Ichikawa, M.J. Shiro, Chem. Soc. Parkin Trans. 2 (2000) 17–26.
[21] (a) B.K. Singh, R.K. Sharma, B.S. Garg, J. Therm. Anal. Cal. 84 (2006) 593–600;
(b) B.K. Singh, N. Bhojak, P. Misra, B.S. Garg, Spectrochim. Acta A 70 (2008) 758–765.
[22] A.W. Coats, J.P. Redfern, Nature 68 (1964) 201–202.
[23] B.K. Singh, R.K. Sharma, B.S. Garg, Spectrochim. Acta A 63 (2006) 96–102.
[24] B.K. Singh, P. Mishra, B.S. Garg, Spectrochim. Acta A 69 (2008) 361–370.
[25] T. Ahamad, N. Nishat, S. Parveen, J. Coord. Chem. 61 (2008) 1963–1972.